

Theoretical insights into the surface growth of rutile TiO₂

Raphael Shirley¹, Jethro Akroyd¹, Luke A. Miller¹, Oliver Inderwildi²,
Uwe Riedel³, and Markus Kraft¹.

released: January 14, 2011

¹ Department of Chemical Engineering
and Biotechnology
University of Cambridge
New Museums Site
Pembroke Street
Cambridge CB2 3RA
United Kingdom
E-mail: mk306@cam.ac.uk

² Smith School of Enterprise
and the Environment
University of Oxford
Hayes House
75 George Street
Oxford OX1 2BQ
United Kingdom

³ Institut für Verbrennungstechnik
Deutsches Zentrum für Luft und Raumfahrt
Universität Stuttgart
Pfaffenwaldring 38-40
70569 Stuttgart
Germany

Preprint No. 100



UNIVERSITY OF
CAMBRIDGE

Keywords: titanium dioxide, surface growth, rutile, TiO₂, TiCl₄

Edited by

Computational Modelling Group
Department of Chemical Engineering and Biotechnology
University of Cambridge
New Museums Site
Cambridge CB2 3RA
United Kingdom

Fax: + 44 (0)1223 334796

E-Mail: c4e@cam.ac.uk

World Wide Web: <http://como.cheng.cam.ac.uk/>



Abstract

Adsorption of TiCl_4 molecules on the reduced $[1\ 1\ 0]$ surface of TiO_2 is investigated using density functional theory with plane wave basis sets and pseudopotentials. Adsorption energies and barriers are calculated and discussed. The rate of this adsorption process is calculated using transition state theory with estimated vibrational frequencies. Derived activation energies are within error bounds of the experimental activation energy for surface growth, consistent with the hypothesis that TiCl_4 adsorption is the rate limiting step to growth. However, quantitative predictions of the rate can not be made based on these theoretical calculations alone, due to sensitive dependence on the vibrational frequencies. Building on the theoretical work presented here and previous experimental results a new kinetic model is constructed consisting of a TiCl_4 adsorption step followed by a secondary reaction with gaseous O_2 . Simulations of a plug flow reactor are used to fit the kinetic constants for the rate limiting adsorption step. Unlike the previous phenomenological models, this new Eley-Rideal model is under the theoretical limit at all conditions and contains a physically motivated dependence on gas phase concentrations.

Contents

1	Introduction	3
2	Computational method	5
2.1	General parameters	5
2.2	Boundary conditions	6
3	First-principles investigations	7
3.1	The structure of adsorbed TiCl_4	8
3.2	The energetics and kinetics of TiCl_4 adsorption	9
3.2.1	Adsorption energy	9
3.2.2	Energy barrier	9
3.2.3	Adsorption rate	11
3.3	Discussion and recommendations	12
4	A kinetic model for surface growth	13
4.1	Oxygen dependence	15
4.2	Simulating a plug flow reactor	16
4.2.1	Parameter estimation and error analysis	17
4.3	Recommended model	19
5	Conclusions	21
	Appendix A; partition functions	24
	Appendix B; limiting rates	26
	Appendix C; model equations	28
	References	30

1 Introduction

Titanium dioxide (TiO_2) is widely used as a pigment, as a catalyst support, and as a photocatalyst. The combustion of titanium tetrachloride (TiCl_4) to synthesise TiO_2 nanoparticles is a multi-million tonne per year industrial process [10]. Typical operating conditions involve purified TiCl_4 being oxidised at high temperatures (1500–2000 K) in a pure oxygen plasma or flame to produce TiO_2 particles [7, 14]. TiO_2 crystallises in three different forms: rutile, anatase and brookite. Rutile is tetragonal and fully described by three parameters: a , c and, u . The parameters a and c are shown in Figure 1, u defines the fractional coordinate of the O atom.

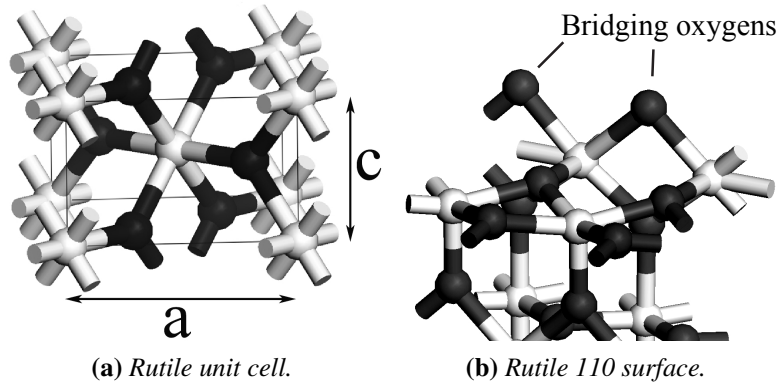


Figure 1: Unit cell of rutile TiO_2 and the stoichiometric $[1\ 1\ 0]$ surface. Titanium atoms are white, oxygen atoms are black. The oxygen atoms at the top of (b) we call bridging oxygen atoms. When there is no oxygen atom present we refer to the site as an oxygen vacancy.

The majority of titania is produced in the rutile form because it is the most stable and has the highest refractive index. These qualities are both crucial for its application as a pigment; gaining the ability to control them is a major technological challenge. The chloride process is well established but we still lack a full understanding of how particles incept and grow. Controlling particle size distributions and other important particle properties depends on a fundamental understanding of particle growth.

This work is concerned with surface growth, the rate of which is not well understood. Simulations conducted so far [24, 26, 37, 39, 45], have relied on the first-order rate expression measured by Ghoshtagore [13] at 673–1020 K:

$$\frac{d N_{\text{TiO}_2}}{d t} = A [\text{TiCl}_4] 4.9 \times 10^3 \text{ cm s}^{-1} \times \exp\left(\frac{-74.8 \text{ kJ/mol}}{k_B T}\right) \quad (1)$$

where N_{TiO_2} is the amount of TiO_2 deposited, A is the surface area, and $[\text{TiCl}_4]$ is the concentration of gas phase TiCl_4 . However, recent work has cast doubt on this rate [46], which is often applied well beyond the conditions at which it was attained. Given the importance of surface growth to the overall synthesis process it is imperative to improve our estimate for the overall rate. Competition between gas phase and surface reaction in the

particle formation process is critical to particle properties [26]; any modelling investigation is dependent on accurate rates. Theoretical investigations have suggested that surface growth may be important in phase determination [33]. Furthermore, additives will likely have an impact on surface growth rates [32, 34, 38] and a detailed molecular model of surface reactions is required to investigate this.

The major experimental conclusion of Ghoshtagore [13] is that an Eley-Rideal model is operating with atomic oxygen as the chemisorbed species and molecular TiCl_4 colliding on the surface from the gas phase. However, the more recent work by Smith et al. [35] claims that the surface can grow by reaction of gaseous O_2 with the reduced surface. They provide useful information about the O_2 adsorption step, arguing that it is reaction of molecular oxygen in the gas phase with Ti^{3+} ions on the surface that is the rate limiting step. The latter work does not suggest a mechanism for taking TiCl_4 out of the gas and is concerned with conditions that are different to those in an industrial reactor given that no TiCl_4 is present. Figure 2 shows the different conditions used in experiments and industry, and highlights the need for a versatile surface growth model.

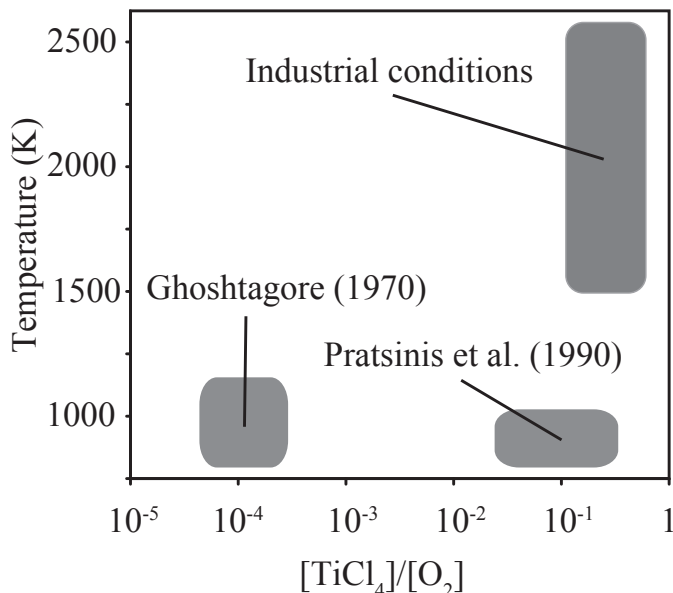


Figure 2: *The work is motivated by concern over the application of the experimentally measured surface growth rates of Ghoshtagore [13] to industrial operating conditions, where it has been applied in previous models.*

The best investigated surface of TiO_2 is [1 1 0]. This is partly because it is the most stable surface and therefore has the largest area on the minimum energy crystal [29]. There are fewer investigations into the other surfaces but key processes may be similar across all faces. The adsorption of H_2O , CO and other species onto this surface has been investigated using Density Functional Theory (DFT) as it is applied in this work [17, 21, 36].

Cl adsorption and desorption on [1 1 0] has been investigated theoretically using DFT [19]. This study was a first attempt at understanding the overall surface growth process.

It mentions the importance of TiCl_4 adsorption but does not investigate it. Since the rate has been found to be first order with respect to TiCl_4 concentration [13], and since this species is the most abundant Ti species at industrial temperatures, its adsorption is likely to be a critical process.

The first aim of this work is to investigate the atomistic processes involved in TiCl_4 adsorption. This will allow us to determine the rough form any kinetic model should take. Comparisons will be made between theoretical rates in limiting cases in order to test current assumptions about surface growth. The second aim is to construct a kinetic model for surface growth. Simulations of particle formation and growth will then be used to fit parameters in this model. This will allow us to provide a kinetic model that is motivated by an understanding of the atomistic processes involved, and capable of reproducing experimentally observed rates. The availability of multiscale models where each process has been validated in this way will facilitate future detailed particle simulations [5, 42], and simulations of nanoparticle formation in reacting flow [1–3, 22].

2 Computational method

This section summarises the theoretical tools used in the paper and details the convergence studies conducted in order to find suitable settings for the calculations. The CASTEP [6] DFT software package is used for all the first-principles work. This uses pseudo-potentials and plane wave basis sets. The calculations are performed using the Perdew-Burke-Ernzerhof (PBE) [25] Generalised Gradient Approximation (GGA) functional. This functional has recently been shown to successfully reproduce bond lengths and energies [33]. Vanderbilt ultra-soft pseudo-potentials [41] are used to represent the core electrons.

2.1 General parameters

This section describes convergence studies with respect to the key calculation parameters; basis set size, and \mathbf{k} -point spacing. All calculations use a basis set cutoff energy of 400 eV which agrees with values found in the literature for similar systems [20]. A cutoff of 400 eV was chosen after a convergence study with respect to surface energies, where errors due to basis set truncation were converged to < 0.01 eV. A $4 \times 4 \times 1$ Monkhorst-Pack grid [23] is used to derive a uniform set of irreducible \mathbf{k} -points in reciprocal space. For transferability between systems of varying size, we refer to the \mathbf{k} -point spacing, which is found to be converged for TiO_2 surface systems at a value of $\leq 0.04 \text{ \AA}^{-1}$ in all spatial directions.

Spin-polarized calculations are used throughout. All the structures investigated changed only slightly when separately optimised for singlet and triplet states. The difference in energy between the optimised geometries at both spin states was uniformly < 0.01 eV.

2.2 Boundary conditions

We use a $\text{Ti}_{24}\text{O}_{48}$ periodic supercell with a 15 Å vacuum slab and six TiO_2 layers. Figure 3 shows convergence of surface energy with respect to number of layers. We are converged in terms of absolute energies to within 0.05 J m^{-2} , which is sufficient for the energy differences we are calculating. Previous studies have restrained lower atoms in order to enforce the bulk geometry, however this leads to a strained cell and could introduce errors in surface energies. We allow all atoms to relax fully. These settings were chosen based on independent convergence tests with respect to surface energy for each parameter. All these convergence criteria are in broad agreement with the recommendations of Kiejna et al. [20].

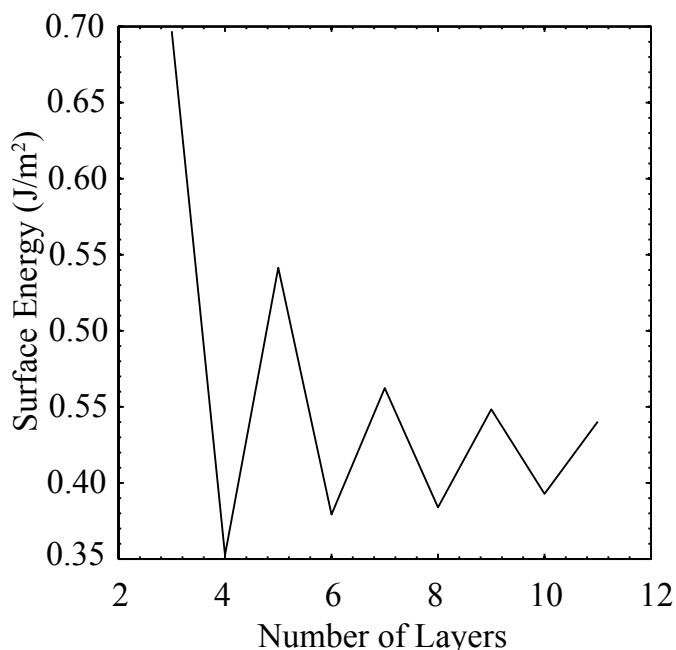


Figure 3: *The calculated surface energy as a function of number of layers. The graph oscillates due to alternating alignment and non-alignment of bridging oxygens. It is possible to estimate the converged value based on only a small number of calculations on smaller films. We are interested in relative values which show weaker dependence on the number of layers.*

The largest source of error is probably due to lateral interaction of TiCl_4 molecules with their image in the neighboring supercell. Figure 4 shows the interaction energy of isolated TiCl_4 molecules with respect to separation. Equation 2 can be used to calculate lateral interaction energy using the data presented in Figure 4.

$$E_{\text{lat}} = \sum_m c_m V_m, \quad (2)$$

where c_m is the number of each interaction type m , and V_m is the energy of the interaction. Each adsorbed TiCl_4 effectively interacts with four adjacent mirror images, two in one direction and two in the other. The total of these four lateral interactions is +12 kJ/mol. It is difficult to ascertain the errors this will introduce to the transition state and adsorption energies. It is possible that lateral interactions will cancel out when the total adsorbed energy is subtracted from the total desorbed energy. Nevertheless, we expect errors of around 12 kJ/mol.

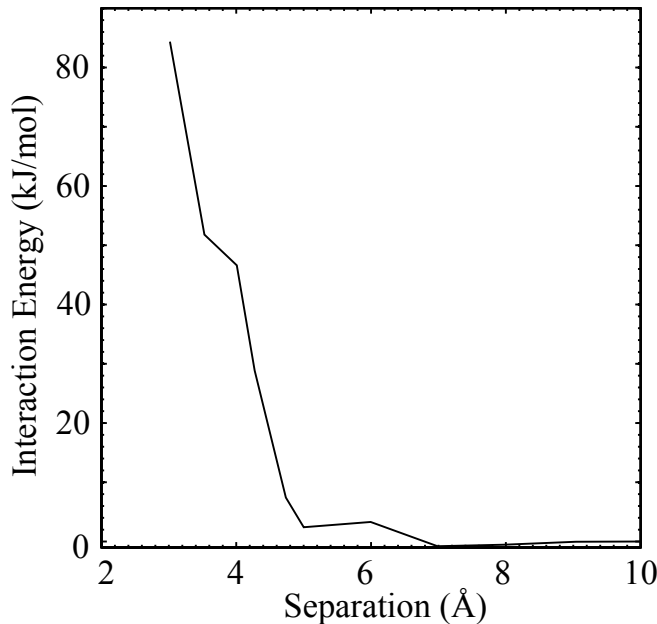


Figure 4: *Interaction energy between two TiCl_4 molecules in a large cell as a function of Ti atom separation from single point calculations. The supercell sizes used here to calculate adsorption energies correspond to slightly under 5 kJ/mol on this plot. Lateral interactions are probably the largest source of error.*

3 First-principles investigations

This section describes investigations in to possible adsorbed structures for TiCl_4 , and calculations of the energetics and rate for TiCl_4 adsorption on to an oxygen vacancy. The aim of this section is to test two hypotheses; that oxygen vacancies are the principle reactive site and that adsorption of TiCl_4 on to them is the rate limiting step.

These hypotheses are made based on some results from the literature. Oxygen vacancies are one of the most common defect sites on rutile [1 1 0] [12]. Many people have suggested they are likely to be important reactive sites [19, 31, 43]. Previous work reports that oxygen coverage is a crucial factor for surface growth [19, 45]. More generally, it is

widely known that the reactivity of any oxide surface depends on the extent to which surface ions are coordination unsaturated [40].

3.1 The structure of adsorbed TiCl_4

We investigated possible adsorbed states by placing TiCl_4 in various configurations around bridging oxygen atoms and vacancy sites, and then optimising the geometry with respect to total energy for the two lowest spin states. Figure 5 shows the only structure for adsorbed TiCl_4 that we found. All the initial configurations we tried either optimised into this chemisorbed state, moved away from the surface, or failed to converge. We could not find a local minimum for TiCl_4 on a bridging oxygen.

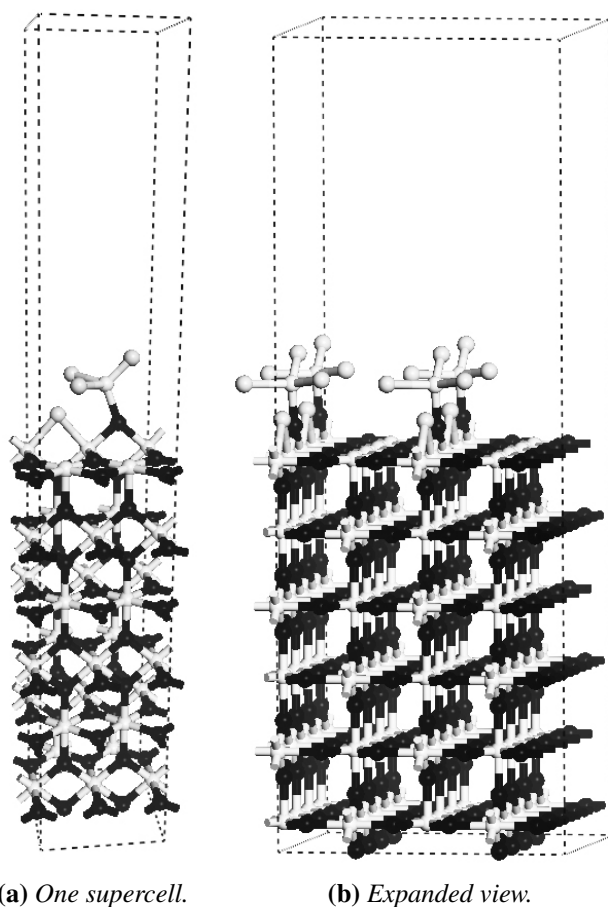


Figure 5: Optimised adsorbate structure shown on a 6 layer supercell. The expanded view demonstrates the proximity of adjacent adsorbed TiCl_4 molecules. Oxygen atoms are black, titanium atoms are white. The TiCl_4 molecule atop the surface is all white.

3.2 The energetics and kinetics of TiCl_4 adsorption

The DFT simulations presented above indicate that vacancies may be a preferential adsorption site. We now investigate the potential energy surface for a gas phase TiCl_4 molecule approaching and adsorbing at one of these vacancy sites. The results of these calculations are used with transition state theory to investigate some limiting cases in order to put bounds on the Arrhenius parameters of this process in an attempt to falsify the hypothesis that it is the rate limiting step.

3.2.1 Adsorption energy

The adsorption energy is calculated using,

$$\Delta E_{\text{adsorption}} = E_{\text{surface + adsorbed species}} - E_{\text{surface + desorbed species}} \quad (3)$$

The adsorption energy from this calculation is -117 ± 12 kJ/mol. The recommended error is based on the scale of lateral interactions calculated in Section 2.2. If lateral interaction energies are similar in the two right hand terms of Equation 3 there will be some cancelation and 12 kJ/mol will be an overestimate of the error. This adsorption process is significantly exothermic. Consider that the initial decomposition of TiCl_4 as measured by Herzler and Roth [18] is endothermic by 387 kJ/mol at 298 K. Given that Pratsinis et al. [27] measures the overall activation energy as 88.8 kJ/mol, TiCl_4 consumption is clearly auto-catalysed by surface growth.

3.2.2 Energy barrier

Energy barriers correspond to saddle points on the potential energy surface. Here, we use the approach of Govind et al. [16] to locate the saddle point involved in the adsorption of TiCl_4 on to an oxygen vacancy. We perform a Linear Synchronous Transit (LST) maximisation followed by a Conjugate Gradient (CG) minimisation. The linear path is based on an initial optimised geometry of TiCl_4 desorbed from the surface and a final geometry of it adsorbed as in Figure 5. Further refinement can be made by performing a Quadratic Synchronous Transit (QST) maximisation followed by a CG minimisation. At the end of each step the average force on nuclei indicates how far from the saddle point the geometry is.

The potential energy surface in these simulations is highly multimodal and finding the saddle point to high accuracy is challenging. Figure 6 shows the result of a single LST/CG step, which gives a barrier of 25 kJ/mol. Alternatively, a further QST/CG step locates a point on the potential energy surface at 43 kJ/mol. However, forces on the atoms after one LST/CG step are lower (0.2 eV/Å) than after the subsequent QST/CG step (0.4 eV/Å), indicating the point at 43 kJ/mol is further from the saddle point where all forces are necessarily zero.

Forces on atoms are lower at the barrier at 25 kJ/mol, and we therefore recommend this value for the barrier but must impose a large error bound of ± 20 kJ/mol on it. This

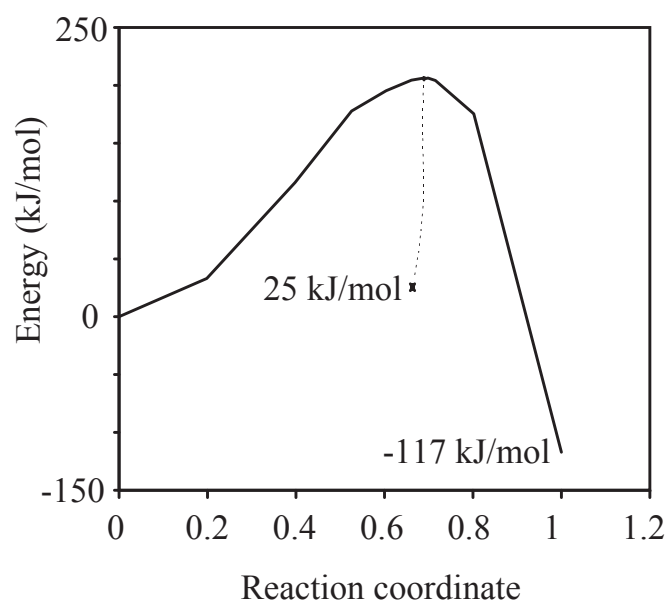


Figure 6: *The energy as a function of reaction coordinate (fractional position along linear path). The main line shows the linear synchronous transit step. The dashed line from the peak of the linear step shows a conjugate gradient step which leads to a significant reduction in energy (from 207 kJ/mol to 25 kJ/mol). The energy scale is defined such that the energy of the desorbed species is 0. Precise energies and geometries are available as CASTEP output files in the Supplemental Material.*

energy barrier of TiCl_4 adsorption on an oxygen vacancy, 25 ± 20 kJ/mol, is a similar order of magnitude albeit lower than the overall, 74.8 kJ/mol, activation energy fitted by Ghoshtagore [13]. Note that when referring to observed/fitted Arrhenius models we speak of an ‘activation energy’, E_a , and when referring to the physical barrier we use the term ‘energy barrier’, E_b . A large part of the observed activation energy comes from the temperature dependence introduced by the partition functions in transition state theory and not from the actual energy barrier. We will now calculate the temperature dependence of the overall rate in order to properly test compatibility with Ghoshtagore [13].

3.2.3 Adsorption rate

Rates of adsorption can be estimated using classical transition state theory,

$$k_{\text{TST}} = \frac{k_{\text{B}}T}{h} \frac{Q^\ddagger}{Q_{\text{rot}}Q_{\text{vib}}(Q_{\text{trans}}/V)} \exp\left(\frac{-E_b}{k_{\text{B}}T}\right), \quad (4)$$

where Q^\ddagger is the partition function of the transition state, $Q_{\text{rot}}Q_{\text{vib}}(Q_{\text{trans}}/V)$ is the partition function of the gaseous species, composed of a rotational (Q_{rot}), vibrational (Q_{vib}), and translational (Q_{trans}/V) contribution, and E_b is the energy barrier to adsorption. The translational partition function is divided by the volume occupied by the molecule, V , in order to give the rate constant in terms of concentrations. When calculating Q_{vib} we take the classical minimum as the zero of energy so that E_b does not require a zero point correction. If we assume that all the transition state modes are vibrations then Q^\ddagger will have five more vibrational modes than Q_{vib} . In order to calculate predictive quantitative rates it might be necessary to consider rotations in the transition state but for the purposes of inspecting bounds on the Arrhenius parameters this assumption is sufficient. All of the partition functions are simple functions of temperature (see Appendix A) and can be found in any statistical mechanics text book [4].

The geometry of the transition state found in the previous section was not sufficiently optimised to give a single imaginary frequency. Despite this inaccuracy it is still possible to consider some limiting cases. If we estimate the new vibrational frequencies of the transition state by assuming they are all equal to the lowest frequency for any molecule investigated in West et al. [44] (14.1 cm^{-1}), and assume the original molecular frequencies are unchanged, we can calculate an order of magnitude estimate for the rate. This estimate will be an upper limit given that we use a low frequency for all the new modes. We calculate k_{TST} over the range 500–1600 K and fit an Arrhenius form ($k = A \exp(E_a/k_{\text{B}}T)$) to it. Figure 7 shows the calculated rate alongside the fitted rate given by Equation 5,

$$k_{\text{TST}} \approx 3 \times 10^{13} \exp\left(\frac{60 \text{ kJ/mol}}{k_{\text{B}}T}\right) \text{ cm}^3 \text{ mol}^{-1} \text{ s}^{-1}. \quad (5)$$

If the same calculations are performed with the upper limit of the barrier, 45 kJ/mol, the corresponding activation energy is calculated as 80 kJ/mol. That is, our calculated activation energy is within error bounds of the Ghoshtagore [13] experimental fit.

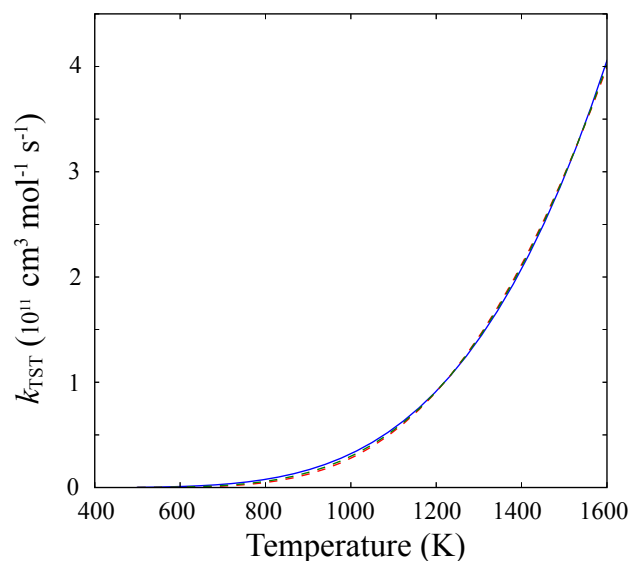


Figure 7: *The calculated rate of adsorption of TiCl_4 on to a bridging oxygen vacancy using estimated frequencies for the transition state (solid blue line), which give an upper limit. The fitted Arrhenius form (dashed red line, $k = A \exp(E_a/k_B T)$) is little improved by a modified Arrhenius form (dashed green line, $k = AT^n \exp(E_a/k_B T)$).*

The transition state found here was quite far from the surface (lowest molecule atom/surface atom separation $> 3 \text{ \AA}$). Based on inspecting the electron density there does not appear to be any bond breaking or formation; the transition state is sufficiently far from the surface that the vibrational modes will be low frequency. However, to be sure our estimated frequencies do not lead to drastically erroneous rates we considered the opposite extreme of high frequency modes. We computed rates by assuming the new vibrational modes take the value of the lowest frequency mode of TiCl_4 (114 cm^{-1}). These bond stretches are significantly higher than modes associated with a physisorbed transition state. This indeed led to rates that were considerably slower. However, there was only moderate impact on the activation energy. Using all combinations of our limiting energy barriers and frequencies produced activation energies between 30 kJ/mol and 80 kJ/mol. The frequencies have a large impact on the pre-exponential factor, but the activation energy is universally higher than the energy barrier by $\approx 30\text{--}35$ kJ/mol regardless of the estimated frequencies. The error in our calculated activation energy is therefore almost entirely due to the error in the energy barrier. Full details of these calculations and limits are given in Appendix B.

3.3 Discussion and recommendations

Until accurate vibrational frequencies can be found it is difficult to give precise, quantitative values for the adsorption rate based on first-principles calculations. However,

calculated activation energies for the adsorption process investigated here agree with the *overall* growth rate of Ghoshtagore [13]. This is consistent with the hypothesis that TiCl_4 adsorption on an oxygen vacancy is the rate limiting step to surface growth. After the TiCl_4 adsorption step, the Cl atoms can desorb leaving Ti^{3+} ions which are free to enter the lattice and subsequently react with molecular oxygen for which Smith et al. [35] observe a 25 kJ/mol barrier. This overall model for the process is in agreement with Rasmussen et al. [30] and Smith et al. [35] and would explain the activated growth process, as well as its order of magnitude compared to the collision limit. This description of surface growth will be used to construct a kinetic model in the next section. The major conclusions of this section are:

- The adsorption energy for TiCl_4 adsorbing on to an oxygen vacancy is -117 ± 12 kJ/mol and the energy barrier is 25 ± 20 kJ/mol.
- Transition state theory calculations using limiting values for the vibrational frequencies indicate that the activation energy for the adsorption rate is 55 ± 25 kJ/mol. We can not impose reasonable bounds on the pre-exponential factor based on these calculations.
- The theoretically calculated activation energies are consistent with the hypothesis that adsorption of TiCl_4 on to an oxygen vacancy site is the rate limiting step during the surface growth of TiO_2 .

4 A kinetic model for surface growth

In this section we build a kinetic model for surface growth based on experimental results from the literature and conclusions from the theoretical work presented in the previous section. There are two basic models for surface growth: Eley-Rideal and Langmuir-Hinshelwood. Ghoshtagore [13] rules out a Langmuir-Hinshelwood mechanism based on the observed temperature and concentration dependence. If the reaction proceeds via an Eley-Rideal model then there are two basic forms to consider: O_2 adsorbs first and reacts with gas phase TiCl_4 , or TiCl_4 adsorbs followed by reaction with O_2 .

Table 1 shows the Ghoshtagore [13] reaction scheme and two possible Eley-Rideal models that give similar rates. In the case of an infinitesimal surface where gas phase concentrations do not change, these processes enable a final state to be reached where surface coverage and TiO_2 growth *rate* both reach a steady state. In order to check these models give similar TiO_2 growth rates, Cantera [15] is used to integrate the corresponding ordinary differential equations and calculate this final rate. We define the quasi-steady state to be reached when the surface growth rate does not change by more than $10^{-5} \mu\text{m s}^{-1}$ over a period of 0.1 ms. These quasi-steady state growth rates are frequently good approximations of actual growth rates due to the time scales concerned being considerably shorter than time scales involving variations of gas phase species concentrations [8]. Appendix C gives an overview of the ordinary differential equations which derive from an Eley-Rideal model with TiCl_4 adsorption first.

Table 1: Simple reaction schemes that could be used to model growth. (g) and (s) signify gas and solid species respectively. S^* is used to represent a generic reactive surface site, $TiCl_4^*$ and O_2^* represent adsorbed $TiCl_4$ and O_2 . We assume S^* to be a bridging oxygen vacancy but it makes no difference to the macroscopic behaviour of the model. Rate constants are calculated based on 100% coverage of reactive sites and a surface site density of $9.43 \times 10^{-10} \text{ mol cm}^{-2}$ from calculated lattice constants [33].

#	Reaction	$k = A T^n \exp(-E_a/k_B T)$		
		A $\text{cm}^3 \text{mol}^{-1} \text{s}^{-1}$	n -	E_a kJ/mol
Model A: Ghoshtagore (zero order with respect to O_2):				
1	$TiCl_4(g) + S^* + O_2(g) \longrightarrow TiO_2(s) + 2 Cl_2(g) + S^*$	5.2×10^{12}	0	74.8
Model B: Eley-Rideal with O_2 adsorption first:				
1	$O_2(g) + S^* \longrightarrow O_2^*$	6.8×10^{11}	$\frac{1}{2}$	0.0
2	$O_2^* + TiCl_4(g) \longrightarrow TiO_2(s) + S^* + 2 Cl_2(g)$	5.2×10^{12}	0	74.8
Model C: Eley-Rideal with O_2 adsorption second:				
1	$TiCl_4(g) + S^* \longrightarrow TiCl_4^*$	5.2×10^{12}	0	74.8
2	$O_2(g) + TiCl_4^* \longrightarrow TiO_2(s) + 2 Cl_2(g) + S^*$	6.8×10^{11}	$\frac{1}{2}$	0.0

4.1 Oxygen dependence

Ghoshtagore [13] suggests that O_2 adsorbs first based on some limiting case observations of the behaviour of the growth rate. He observed that at low O_2 concentrations,

$$\frac{d N_{TiO_2}}{d t} \propto A [TiCl_4(g)] [O_2(g)]^{1/2}, \quad (6)$$

but at high O_2 concentrations,

$$\frac{d N_{TiO_2}}{d t} \propto A [TiCl_4(g)], \quad (7)$$

where A is the surface area. We suggest an alternative interpretation of this observation; the process that removes O_2 from the gas phase is fast compared to the corresponding process for $TiCl_4$. One can construct two mechanisms which show the same behaviour, one with O_2 chemisorption first followed by reaction with $TiCl_4$ and another with the opposite ordering. Models B and C in Table 1 produce identical rates after they have been integrated to quasi-steady state constant coverages. When the oxygen adsorption rate is collision limited, models B and C behave identically to model A except at low O_2 concentrations.

Ghoshtagore [13] defines a ‘critical oxygen partial pressure’, given by $p_{O_2_{crit}} \propto (p_{TiCl_4})^3$, below which there is half order oxygen dependence. Defining the oxygen dependence in this way is equivalent to giving the reaction an order of $-3/2$ with respect to $TiCl_4$. Figure 8 shows the behaviour of both the original rate and that with his recommended oxygen dependence. The difference becomes large at industrial concentrations where the growth rate with half order O_2 dependence becomes low. Extrapolation of this model to industrial conditions is not recommended.

This discussion has focused on what assumptions about the kinetic model can be made based on previous experimental investigations. The key results we take from these investigations are:

- Ghoshtagore [13] observes that surface growth shows half order dependence on oxygen concentration at low oxygen concentrations and is zero order in oxygen otherwise. From this result we argue that the process removing O_2 from the gas phase is fast compared to the corresponding process for $TiCl_4$.
- This oxygen dependence could be modelled by two equivalent Eley-Rideal models. It is well established that the surface is usually reduced [9], and Smith et al. [35] show that a reduced surface can grow by reaction with gaseous O_2 . This suggests a model with $TiCl_4$ adsorption first.
- The mathematical form given by Ghoshtagore [13] for half order oxygen dependence can not be extrapolated beyond the low $TiCl_4$ concentrations used in his experiments.

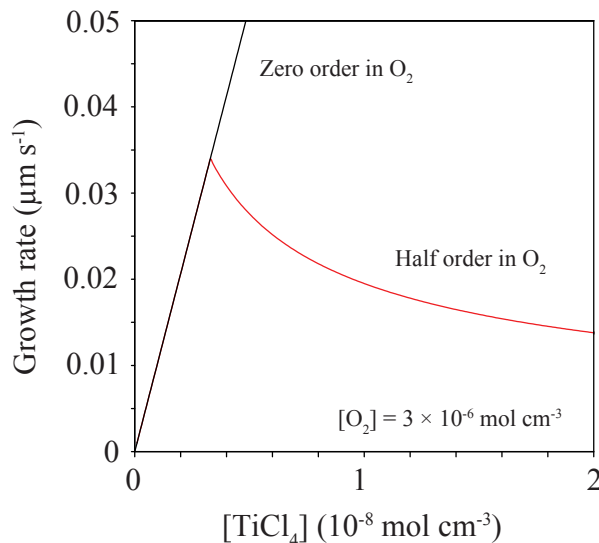


Figure 8: *The surface growth rate as a function of $[\text{TiCl}_4]$ for the Ghoshtagore [13] model. The black line shows how it has typically been applied with zero order oxygen dependence. The red line shows the modified rate with half order oxygen dependence. This is shown at relatively low concentrations of TiCl_4 . As $[\text{TiCl}_4]$ increases the difference becomes large.*

4.2 Simulating a plug flow reactor

The work presented in this paper was originally motivated by the failure of previous simulations [46] to reproduce the observations of Pratsinis et al. [27]. In this section, we investigate the impact of surface growth rates on these simulations using the moment method with interpolative closure to solve the population balance and couple it to the gas phase chemistry. This method is an inexpensive alternative to stochastic population balance solvers. It does not provide such detailed information about particles but has recently been shown to agree with stochastic simulations in terms of overall rates and low-order moments of the resulting size distributions [11].

The original Pratsinis et al. [27] investigation measured the reaction of $[\text{O}_2]/[\text{TiCl}_4] = 5$ in argon (99% by volume) in a tube, with an internal diameter of 1/8 inch, heated to 973 – 1273 K. Pratsinis et al. [27] calculate an effective rate constant for the overall oxidation kinetics of TiCl_4 vapour,

$$k_{\text{eff}} = -\frac{\ln(C_o/C_i)}{t}, \quad (8)$$

assuming the reaction is first-order in TiCl_4 with Arrhenius kinetics and where C_i and C_o are the measured inlet and outlet TiCl_4 concentrations and t is residence time in the isothermal zone of the reactor. This experiment was modelled using an imposed temperature profile taken from Pratsinis et al. [27], Figure 3.

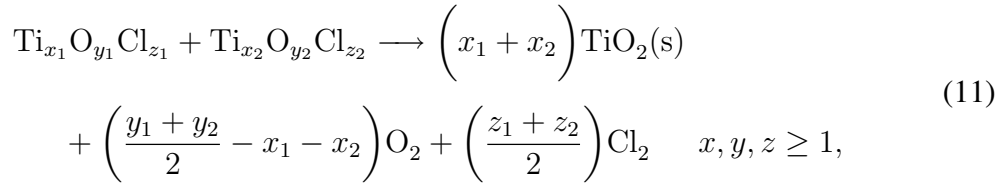
For the purpose of fitting we adopt the simple one step surface growth model,



with varying order, m , with respect to $\text{O}_2(\text{g})$:

$$\frac{d[\text{TiO}_2(\text{s})]}{dt} = k_{\text{fit}} [S^*] [\text{TiCl}_4(\text{g})] [\text{O}_2(\text{g})]^m. \quad (10)$$

We use this phenomenological form so that reaction order with respect to oxygen can be investigated. Agreement could only be obtained by changing both the particle inception model and the surface growth rate. The inception model of West et al. [46] is based on the collision limited reaction of all titanium species containing two or more Ti atoms. This inception model was flawed in that reactions forming $\text{Ti}_3\text{O}_x\text{Cl}_y$ species were not considered despite the fact that the smallest ‘particle’ in the population balance model was Ti_4O_8 . We use a new inception model to give an upper limit on the inception rate. The new model is based on collision limited reactions of any pair of titanium oxychlorides as defined in Equation 11.



where, the collision diameter is taken as 0.65 nm. This is the next fastest inception model after allowing collision limited dimerisation of TiCl_4 (which gives rates that are much too high), and gives some confidence that the fitted surface growth rate will not be an overestimate. We also rule out the possibility of significant errors due to surface areas that are too low because there is negligible difference in the overall rate between the zero sintering (maximum surface area) simulations of West et al. [46] and comparable infinite sintering (minimum surface area) simulations conducted here.

4.2.1 Parameter estimation and error analysis

We used simulations of the plug flow reactor of Pratsinis et al. [27] to optimise the Arrhenius parameters of the overall surface growth rate of Equation 10.

Figure 9 shows the behaviour of some of the older models along with the new modified and fitted model. The original model of West et al. [46] is barely distinguishable from simulations which ignore particle inception altogether; the consumption of TiCl_4 is essentially negligible. Since the gas kinetics have been shown to compare favorably to short time-scale rapid compression machine experiments [28, 46] and are rate limited by well established experimental rates from shock tube experiments [18] we conclude that it is the particle processes that were too slow in the simulations of West et al. [46].

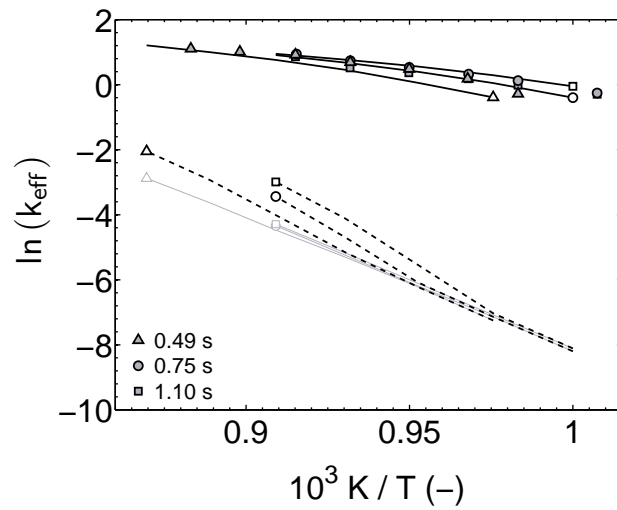


Figure 9: Arrhenius plot of the plug flow reactor results of Pratsinis et al. [27] (filled shapes). Also shown are simulations of the full particle formation process using a number of possible models. The light grey lines show simulation results using only the gas kinetic part of the model presented by West et al. [46]. The dashed lines show simulation using the full model presented by West et al. [46]. The solid lines passing through the experimental data points show simulations with inception processes based on Equation 11, and surface growth rate fitted to the Pratsinis et al. [27] data.

Achieving a good fit in Figure 9 was weakly dependent on both the temperature dependence of the surface growth rate and the order, m , with respect to oxygen. We investigated some limiting cases in an attempt to measure the errors associated with the fitting procedure. The values associated with these cases are shown in Table 4. The table shows a pseudo rate constant $k'_{\text{fit}} = k_{\text{fit}} \times [\text{O}_2(\text{g})]^m$ at 1050 K for all of the fits and demonstrates a similar rate in all cases. It follows that we can only make statements regarding ranges for the activation energy and pre-exponential factor. The pseudo rate constant for the Ghoshtagore [13] model at 1050 K is $1 \times 10^9 \text{ cm}^3 \text{ mol}^{-1} \text{ s}^{-1}$, seven times smaller than the fitted rates.

Table 2: *Limiting values for the Arrhenius parameters based on fitting the rate constant to Pratsinis et al. [27]. The order with respect to O_2 concentration, m , has negligible impact on the fit. A pseudo rate constant $k'_{\text{fit}} = k_{\text{fit}} \times [\text{O}_2(\text{g})]^m$ is shown at 1050 K to demonstrate the equivalence of the reaction rates at a typical simulation temperature. Rate constants are calculated based on 100% coverage of reactive sites and a surface site density of $9.43 \times 10^{-10} \text{ mol cm}^{-2}$.*

Limiting case	m	$k_{\text{fit}} = A \exp(-E_a/k_{\text{B}}T)$		k'_{fit} $\text{cm}^3 \text{ mol}^{-1} \text{ s}^{-1}$
		A $(\text{cm}^3 \text{ mol}^{-1})^{m+1} \text{ s}^{-1}$	E_a kJ/mol	
Low A fit	0	2.3×10^{11}	32	6.1×10^9
High A fit	0	1.1×10^{13}	64	7.3×10^9
Low A fit	$\frac{1}{2}$	2.1×10^{15}	40	6.9×10^9
High A fit	$\frac{1}{2}$	2.7×10^{15}	43	6.4×10^9
Low A fit	1	2.1×10^{18}	30	6.8×10^9
High A fit	1	2.1×10^{19}	50	6.9×10^9

The fitted activation energies, $50 \pm 20 \text{ kJ/mol}$, are similar to those from the theoretically calculated rates, $55 \pm 25 \text{ kJ/mol}$, in Section 3.2.3. There is a factor of 10 difference in k'_{fit} , between the limiting cases in Table 4 when extrapolated to 2000 K. These extremes are 1/2 and 5 times the Ghoshtagore [13] rate at 2000 K. Since oxygen is in five fold excess similar fits are achieved with $m = 0, 1/2, 1$. Conclusions about the relative order with respect to oxygen can not be made based on this data.

4.3 Recommended model

Building on these new fits and the restrictions on the form suggested by the theoretical investigations, we suggest a kinetic model for future simulations in Table 3. This shows the Eley-Rideal kinetic model in which the TiCl_4 adsorption rate is set to give growth rates equal to the fitted reactions in Table 4. Figure 10 shows the steady state growth rate of this model as a function of $\text{TiCl}_4(\text{g})$ concentration at a number of $\text{O}_2(\text{g})$ concentrations. The secondary O_2 reaction is given the collision limited rate multiplied by an exponential

sticking probability using the activation energy measured by Smith et al. [35]. This step is considerably faster than the rate limiting TiCl_4 adsorption step. At stoichiometric concentrations, coverage of S^* is over 98% at the quasi-steady state, and the model behaves like a one step model. Only at low O_2 concentration does the coverage of TiCl_4^* become appreciable. This goes some way to explain the non linear dependence on oxygen concentration. Further insight into the pre-exponential factor for the O_2 adsorption step would allow the model to be applicable in the full range of TiCl_4/O_2 concentration regimes.

Table 3: *The recommended kinetic model with a TiCl_4 adsorption rate found by fitting the overall surface growth rate to Pratsinis et al. [27]. (g) and (s) signify gas, and solid phases respectively. S^* is used to represent a generic reactive surface site, TiCl_4^* represents adsorbed TiCl_4 . Rate constants are calculated based on 100% coverage of reactive sites and a surface site density of $9.43 \times 10^{-10} \text{ mol cm}^{-2}$. The model is available in Cantera format [15] as Supplemental Material.*

#	Reaction	$k = A T^n \exp(-E_a/k_B T)$		
		A $\text{cm}^3 \text{ mol}^{-1} \text{ s}^{-1}$	n -	E_a kJ/mol
1	$\text{TiCl}_4(\text{g}) + \text{S}^* \xrightarrow{k_1} \text{TiCl}_4^*$	2.1×10^{12}	0	50
2	$\text{TiCl}_4^* + \text{O}_2(\text{g}) \xrightarrow{k_2} \text{TiO}_2(\text{s}) + 2 \text{Cl}_2(\text{g}) + \text{S}^*$	6.8×10^{11}	$\frac{1}{2}$	25

Table 4 demonstrates that the data can be fitted using many A/E_a combinations. The particular fit was chosen so as to have an activation energy that was central to the range given in Table 4. Table 3 shows the Arrhenius parameters we present based on assuming 100% coverage of reactive sites and a surface site density of $9.43 \times 10^{-10} \text{ mol cm}^{-2}$. Obviously, if further insight into the coverage of oxygen vacancies becomes available the fitted rates must be adjusted accordingly. Given the wide range of Arrhenius parameters that gave good fits the recommended rate is only valid in this temperature range.

The multiscale model is highly non-linear and it is difficult to ascertain rates of individual processes using optimisation techniques. This is a critical issue for the community to resolve because the relative rates of gas kinetics, inception, and surface growth determine particle properties such as the particle size distribution. More work needs to be done to understand the relative rates of all the processes involved. While these parameter fitting studies do not provide a fine degree of accuracy, they are useful for investigating the *relative* rates of important processes and highlight the incompatibility between the surface growth rate of Ghoshtagore [13], the reaction rates of Herzler and Roth [18], and the inception model of West et al. [46]. The main conclusions of this section are:

- The fitted activation energy for TiCl_4 adsorption is $50 \pm 20 \text{ kJ/mol}$, which agrees with the theoretically calculated value of $55 \pm 25 \text{ kJ/mol}$. The pre-exponential factor is $2.1 \times 10^{12} \text{ cm}^3 \text{ mol}^{-1} \text{ s}^{-1}$ to within a factor of ten.
- We can not fit the rate of oxygen adsorption based on the data in this paper. We

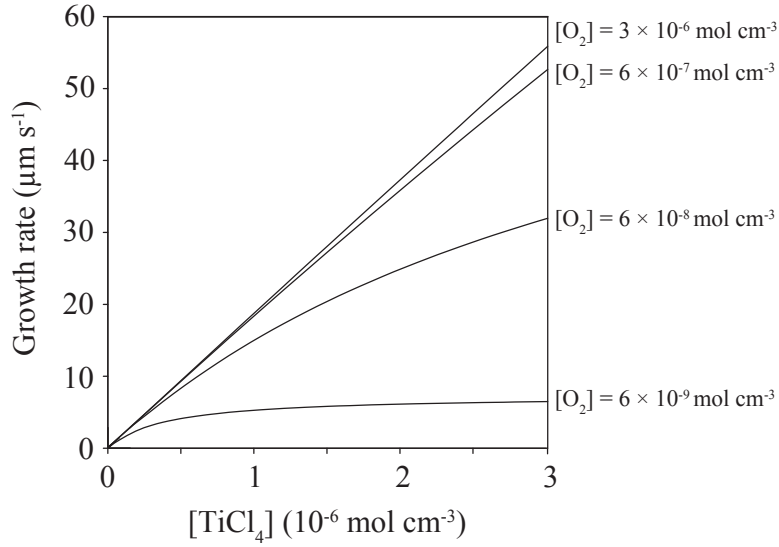


Figure 10: *Quasi-steady state growth rate of the recommended model (defined in Table 3) at 2000 K and atmospheric pressure, as a function of $[\text{TiCl}_4]$. TiCl_4 concentration is varied at a number of fixed O_2 concentrations. The remaining gas is argon.*

therefore assume a collision limited reaction with an exponential sticking probability based on the experimental investigation of Smith et al. [35].

- For future simulations, we recommend the kinetic model for surface growth shown in Table 3.

5 Conclusions

We have presented a first-principles study into the adsorption of TiCl_4 on the $[1\ 1\ 0]$ surface of rutile TiO_2 . Based on these results and previous experimental observations, we suggest a new kinetic model for surface growth. This model reflects atomistic processes and behaves in subtle but crucially different ways to previous phenomenological models. We simulated a plug flow reactor experiment from the literature using the moment method with interpolative closure to solve the particle population balance and couple it to the gas kinetic model. A parameter optimisation procedure allowed us to recommend a rate for the TiCl_4 adsorption reaction in the new model. This work leads to the following conclusions:

- The adsorption energy of TiCl_4 onto a bridging oxygen vacancy is -117 ± 12 kJ/mol, with an energy barrier of 25 ± 20 kJ/mol. The rate of this adsorption was calculated using transition state theory with estimated vibrational frequencies. These calculations are consistent with the hypothesis that adsorption of TiCl_4 on to an oxygen vacancy is the rate limiting step to surface growth.

- Comparisons between previous and possible surface growth models indicate that an Eley-Rideal model with TiCl_4 adsorption first is appropriate.
- The surface growth of TiO_2 can be explained using an Eley-Rideal model, with a TiCl_4 adsorption rate fitted to experiment. The activation energy for this TiCl_4 adsorption process is 50 ± 20 kJ/mol. This new model incorporates a physically reasonable dependence on both O_2 and TiCl_4 concentrations when coupled to the existing gas kinetic model.

Acknowledgments

We thank Tioxide Europe Limited for the financial support of Raphael Shirley and Luke Miller, reSolutions Ltd and the EPSRC (EP/C537564/1) for the financial support of Jethro Akroyd, and the Martin Smith Foundation for the financial support of Oliver Inderwildi. We thank Heidelberg University for providing generous access to the HELICS high performance computing system.

Appendix A

Here, we specify the partition functions used for the calculation of k_{TST} . The partition function, Q , is defined by the following sum over the microscopic energy states, i ,

$$Q = \sum_i g_i \exp\left(\frac{E_i}{k_{\text{B}}T}\right), \quad (12)$$

where g_i is the degeneracy, and E_i the energy, of state i . The specific partition functions used to calculate adsorption rates are given below. The translational partition function is,

$$Q_{\text{trans}} = \left(\frac{2\pi mk_{\text{B}}T}{h^2}\right)^{\frac{3}{2}} V, \quad (13)$$

where m is the molecular mass, and V is the volume occupied by the molecule. The vibrational partition functions, with the zero of energy at the classical minimum, are given by

$$Q_{\text{rot}}^{\ddagger}, Q_{\text{vib}} = \prod_n \left(\frac{\exp(hf_n/2k_{\text{B}}T)}{1 - \exp(hf_n/k_{\text{B}}T)}\right), \quad (14)$$

where f_n is the frequency of mode n . The rotational partition function is given by,

$$Q_{\text{rot}} = \frac{8\pi^2 (8\pi^3 I_x I_y I_z)^{1/2} (k_{\text{B}}T)^3}{\sigma h^3}, \quad (15)$$

where I_x, I_y , and I_z are the principal moments of inertia and σ is the symmetry factor. These are used to calculate

$$k_{\text{TST}} = \frac{k_{\text{B}}T}{h} \frac{Q_{\text{rot}}^{\ddagger}}{Q_{\text{rot}} Q_{\text{vib}} (Q_{\text{trans}}/V)} \exp\left(\frac{-E_{\text{b}}}{k_{\text{B}}T}\right), \quad (16)$$

at different temperatures and an Arrhenius form is fitted to the results. The above form for the rate comes from the Eyring equation,

$$k_{\text{TST}} = \frac{k_{\text{B}}T}{h} \exp\left(\frac{-\Delta G^{\ddagger}}{k_{\text{B}}T}\right), \quad (17)$$

which is derived from assuming a quasi-equilibrium between the activated complex and the reactants and using statistical mechanics to calculate the equilibrium coefficient. The central argument of this derivation is that even if the reactants and products are not at equilibrium the concentration of activated complexes does not change.

In the modified Arrhenius equation with $n = 1$,

$$k = AT \exp\left(\frac{-E_{\text{a}}}{k_{\text{B}}T}\right), \quad (18)$$

E_a is not equal to ΔG^\ddagger because ΔG^\ddagger is a function of T .

Appendix B

Here, we show a typical calculation of k_{TST} , from the values used in the paper. For TiCl_4 ,

$$\begin{aligned} I_x, I_y, I_z &= 1576 \text{ amu bohr}^2, \\ f_{\text{TiCl}_4} &= (114, 114, 134, 134, 134, 386, 496, 496, 496) \text{ cm}^{-1}, \\ \sigma &= 12, \\ m &= 189.679 \text{ amu}. \end{aligned}$$

For the transition state, we take a limiting value for the five new modes and assume the original TiCl_4 modes do not change,

$$\begin{aligned} f_{\text{est}} &= 14.1 \text{ cm}^{-1}, \\ f^\ddagger &= f_{\text{TiCl}_4} \oplus (f_{\text{est}}, f_{\text{est}}, f_{\text{est}}, f_{\text{est}}, f_{\text{est}}) \\ &= (114, 114, 134, 134, 134, 386, 496, 496, 496, 14.1, 14.1, 14.1, 14.1, 14.1) \text{ cm}^{-1}. \end{aligned}$$

Using these values we can calculate the partition functions at a given temperature. Since the molecular frequencies do not change, the partition functions derived from them cancel in Equation 4 and they do not affect the rate. At 1000 K,

$$\begin{aligned} Q^\ddagger &= 7.0 \times 10^{12}, \\ (Q_{\text{trans}}/V) &= 1.6 \times 10^{34} \text{ m}^{-3}, \\ Q_{\text{rot}} &= 3.8 \times 10^5, \\ Q_{\text{vib}} &= 2.4 \times 10^4, \\ Q_{\text{rot}} Q_{\text{vib}} (Q_{\text{trans}}/V) &= 1.4 \times 10^{44} \text{ m}^{-3}, \\ \frac{Q^\ddagger}{Q_{\text{rot}} Q_{\text{vib}} (Q_{\text{trans}}/V)} &= 5.1 \times 10^{-32} \text{ m}^3, \\ &= 3.2 \times 10^{-8} \text{ m}^3 \text{ mol}^{-1}, \\ \frac{k_{\text{B}} T}{h} &= 2 \times 10^{13} \text{ s}^{-1}, \\ \exp\left(\frac{25 \text{ kJ/mol}}{k_{\text{B}} T}\right) &= 0.05, \\ k_{\text{TST}} &= 3.2 \times 10^{10} \text{ cm}^3 \text{ mol}^{-1} \text{ s}^{-1}. \end{aligned}$$

If we change f_{est} to 114 cm^{-1} , then $k_{\text{TST}} = 9 \times 10^5 \text{ cm}^3 \text{ mol}^{-1} \text{ s}^{-1}$ at 1000 K. Using the bounds on the energy barrier from the DFT calculations and physical limits on the new vibrational frequencies,

$$14.1 \text{ cm}^{-1} < f_{\text{est}} < 114 \text{ cm}^{-1},$$

$$5 \text{ kJ/mol} < E_{\text{b}} < 45 \text{ kJ/mol},$$

we can calculate propagated bounds on the activation energy. All the extremes are given in the following table.

Table 4: *Limiting values for the energy barrier and new transition state modes along with rates calculated using transition state theory. A characteristic rate constant is shown at 1000 K as are values for the Arrhenius parameters fitted over the temperature range 500–1600 K.*

f_{est} cm^{-1}	E_{b} kJ/mol	k_{TST} at 1000 K $\text{cm}^3 \text{ mol}^{-1} \text{ s}^{-1}$	$k_{\text{Arr}} = A \exp(-E_{\text{a}}/k_{\text{B}}T)$	
			A $\text{cm}^3 \text{ mol}^{-1} \text{ s}^{-1}$	E_{a} kJ/mol
14.1	25	3×10^{10}	3×10^{13}	60
14.1	45	3×10^9	4×10^{13}	80
14.1	5	4×10^{11}	3×10^{13}	36
114	25	9×10^5	1×10^9	60
114	45	8×10^4	1×10^9	80
114	5	1×10^7	8×10^8	37

Appendix C

This section shows the set of ordinary differential equations that derive from the recommended Eley-Rideal model. If the available surface area per unit volume does not change they are,

$$\frac{d[\text{TiCl}_4^*]}{dt} = k_1 [\text{TiCl}_4(\text{g})] [\text{S}^*] - k_2 [\text{TiCl}_4^*] [\text{O}_2(\text{g})], \quad (19)$$

$$\frac{d[\text{S}^*]}{dt} = -k_1 [\text{TiCl}_4(\text{g})] [\text{S}^*] + k_2 [\text{TiCl}_4^*] [\text{O}_2(\text{g})], \quad (20)$$

$$\frac{d[\text{TiCl}_4(\text{g})]}{dt} = -k_1 [\text{TiCl}_4(\text{g})] [\text{S}^*], \quad (21)$$

$$\frac{d[\text{O}_2(\text{g})]}{dt} = -k_2 [\text{TiCl}_4^*] [\text{O}_2(\text{g})], \quad (22)$$

$$\frac{d[\text{Cl}_2(\text{g})]}{dt} = 2k_2 [\text{TiCl}_4^*] [\text{O}_2(\text{g})], \quad (23)$$

$$\frac{d[\text{TiO}_2(\text{s})]}{dt} = -k_2 [\text{TiCl}_4^*] [\text{O}_2(\text{g})]. \quad (24)$$

If all concentrations are known at some time t_0 ,

$$\begin{aligned} [\text{TiCl}_4^*](t_0) &= [\text{TiCl}_4^*]_0, \\ [\text{S}^*](t_0) &= [\text{S}^*]_0, \\ [\text{TiCl}_4(\text{g})](t_0) &= [\text{TiCl}_4(\text{g})]_0, \\ [\text{O}_2(\text{g})](t_0) &= [\text{O}_2(\text{g})]_0, \\ [\text{Cl}_2(\text{g})](t_0) &= [\text{Cl}_2(\text{g})]_0, \\ [\text{TiO}_2(\text{s})](t_0) &= [\text{TiO}_2(\text{s})]_0, \end{aligned}$$

then one can formulate an initial value problem and integrate the time dependent concentrations. The initial values along with the original ODEs provide a complete description of the mathematical behavior of the new model. It is often useful to investigate growth rates in a constant gas phase environment. In that case the equations become,

$$\frac{d[\text{TiCl}_4^*]}{dt} = k_1 [\text{TiCl}_4(\text{g})] [\text{S}^*] - k_2 [\text{TiCl}_4^*] [\text{O}_2(\text{g})], \quad (25)$$

$$\frac{d[\text{S}^*]}{dt} = -k_1 [\text{TiCl}_4(\text{g})] [\text{S}^*] + k_2 [\text{TiCl}_4^*] [\text{O}_2(\text{g})], \quad (26)$$

$$\frac{d[\text{TiCl}_4(\text{g})]}{dt} = \frac{d[\text{O}_2(\text{g})]}{dt} = \frac{d[\text{Cl}_2(\text{g})]}{dt} = 0, \quad (27)$$

$$\frac{d[\text{TiO}_2(\text{s})]}{dt} = -k_2 [\text{TiCl}_4^*] [\text{O}_2(\text{g})]. \quad (28)$$

Equations 25–28 integrate to the quasi-steady state shown in Figure 10. When the surface growth model is coupled to the existing gas kinetic model or a population balance solver then new terms are introduced into the right hand sides of Equations 19–24

References

- [1] J. Akroyd, A. J. Smith, L. R. McGlashan, and M. Kraft. Comparison of the stochastic fields method and DQMoM-IEM as turbulent reaction closures. *Chemical Engineering Science*, 65(20):5429–5441, 2010. ISSN 0009-2509. doi:10.1016/j.ces.2010.06.039. URL <http://www.sciencedirect.com/science/article/B6TFK-50GJ2PT-6/2/06b608a76d00af0fa6b5baeab2fe77a6>.
- [2] J. Akroyd, A. J. Smith, L. R. McGlashan, and M. Kraft. Numerical investigation of DQMoM-IEM as a turbulent reaction closure. *Chemical Engineering Science*, 65(6):1915–1924, 2010. ISSN 0009-2509. doi:10.1016/j.ces.2009.11.010. URL <http://www.sciencedirect.com/science/article/B6TFK-4XRCRV6-4/2/db9ab84b5e9f67325f8fdc23e73d7842>.
- [3] J. Akroyd, A. J. Smith, R. Shirley, L. R. McGlashan, and M. Kraft. A coupled CFD-population balance approach for nanoparticle synthesis in turbulent reacting flows. c4e-Preprint Series (<http://como.cheng.cam.ac.uk>) Technical Report 99, c4e-Preprint Series, Cambridge, 2010.
- [4] P. Atkins. *Physical Chemistry*. Oxford University Press, 1998.
- [5] M. Celnik, R. Patterson, M. Kraft, and W. Wagner. A predictor-corrector algorithm for the coupling of stiff odes to a particle population balance. *Journal of Computational Physics*, 228(8):2758–2769, 2009. ISSN 0021-9991. doi:10.1016/j.jcp.2008.12.030. URL <http://www.sciencedirect.com/science/article/B6WHY-4VDS8NP-1/2/1e6b63f14fedcec77b270b15d967e561>.
- [6] S. Clark, M. Segall, C. Pickard, P. Hasnip, M. Probert, K. Refson, and M. Payne. First principles methods using CASTEP. *Z. Kristallogr.*, 220:567–570, May 2005. doi:10.1524/zkri.220.5.567.65075.
- [7] J. C. Deberry, M. Robinson, M. Pomponi, A. J. Beach, Y. Xiong, and K. Akhtar. Controlled vapor phase oxidation of titanium tetrachloride to manufacture titanium dioxide. US Patent 6,387,347, 2002. URL <http://www.google.com/patents?id=r3gKAAAEBAJ>.
- [8] O. Deutschmann. *Computational Fluid Dynamics Simulation of Catalytic Reactors*. Wiley, 2008. doi:10.1002/9783527610044.hetcat0097. URL <http://dx.doi.org/10.1002/9783527610044.hetcat0097>.
- [9] U. Diebold. The surface science of titanium dioxide. *Surf. Sci. Rep.*, 48(5-8):53–229, 2003. doi:10.1016/S0167-5729(02)00100-0.
- [10] J. Emsley. *Molecules at an Exhibition*. Oxford University Press, 1999.

- [11] M. Frenklach. Method of moments with interpolative closure. *Chemical Engineering Science*, 57(12):2229–2239, 2002. ISSN 0009-2509. doi:10.1016/S0009-2509(02)00113-6. URL <http://www.sciencedirect.com/science/article/B6TFK-45KSPWJ-1/2/7afa0c7fd2a64e8f3492d764ecb8decf>.
- [12] M. V. Ganduglia-Pirovano, A. Hofmann, and J. Sauer. Oxygen vacancies in transition metal and rare earth oxides: Current state of understanding and remaining challenges. *Surface Science Reports*, 62(6):219–270, 2007. ISSN 0167-5729. doi:10.1016/j.surfrep.2007.03.002. URL <http://www.sciencedirect.com/science/article/B6TVY-4NVCFPB-1/2/cbeb0d3783ddaff7174dcd93025d26c5>.
- [13] R. N. Ghoshtagore. Mechanism of heterogeneous deposition of thin film rutile. *J. Electrochem. Soc.*, 117:529–534, 1970. doi:10.1149/1.2407561.
- [14] R. A. Gonzalez, C. D. Musick, and J. N. Tilton. Process for controlling agglomeration in the manufacture of TiO₂. US Patent 5,508,015, April 1996. URL <http://www.google.com/patents?id=N80mAAAAEBAJ>.
- [15] D. G. Goodwin. An open source, extensible software suite for CVD process simulation. In M. Allendorff, F. Maury, and F. Teyssandier, editors, *Chemical Vapor Deposition XVI and EUROCVI 14*, volume 2003-08 of *ECS Proceedings*, pages 155–162, Pennington, New Jersey, USA, 2003. The Electrochemical Society, The Electrochemical Society. URL www.cantera.org.
- [16] N. Govind, M. Petersen, G. Fitzgerald, D. King-Smith, and J. Andzelm. A generalized synchronous transit method for transition state location. *Computational Materials Science*, 28(2):250–258, 2003. ISSN 0927-0256. doi:10.1016/S0927-0256(03)00111-3. URL <http://www.sciencedirect.com/science/article/B6TWM-49H73N8-D/2/b91c1b4d9f942a665ad9ec4a082a8351>. Proceedings of the Symposium on Software Development for Process and Materials Design.
- [17] L. A. Harris and A. A. Quong. Molecular chemisorption as the theoretically preferred pathway for water adsorption on ideal rutile TiO₂ (110). *Phys. Rev. Lett.*, 93(8):086105, Aug 2004. doi:10.1103/PhysRevLett.93.086105.
- [18] J. Herzler and P. Roth. Shock tube study of the reaction of H atoms with TiCl₄. *J. Phys. Chem. A*, 101:9341–9343, 1997.
- [19] O. Inderwildi and M. Kraft. Adsorption, Diffusion and Desorption of Chlorine on and from Rutile TiO₂{110}: A Theoretical Investigation. *Chem. Phys. Phys. Chem.*, 8:444–451, 2007. doi:10.1002/cphc.200600653.
- [20] A. Kiejna, T. Pabisiak, and S. Gao. The energetics and structure of rutile TiO₂ [110]. *Journal of Physics: Condensed matter*, 18(17):4207–4217, 2006. doi:10.1088/0953-8984/18/17/009.

- [21] P. J. D. Lindan, N. M. Harrison, and M. J. Gillan. Mixed dissociative and molecular adsorption of water on the rutile (110) surface. *Phys. Rev. Lett.*, 80(4):762–765, Jan 1998. doi:10.1103/PhysRevLett.80.762.
- [22] M. Mehta, Y. Sung, V. Raman, and R. O. Fox. Multiscale modeling of TiO₂ nanoparticle production in flame reactors: Effect of chemical mechanism. *Industrial & Engineering Chemistry Research*, 49(21):10663–10673, 2010. doi:10.1021/ie100560h. URL <http://pubs.acs.org/doi/abs/10.1021/ie100560h>.
- [23] H. J. Monkhorst and J. D. Pack. Special points for brillouin-zone integrations. *Phys. Rev. B*, 13(12):5188–5192, Jun 1976. doi:10.1103/PhysRevB.13.5188.
- [24] N. M. Morgan, C. G. Wells, M. J. Goodson, M. Kraft, and W. Wagner. A new numerical approach for the simulation of the growth of inorganic nanoparticles. *J. Comput. Phys.*, 211(2):638–658, 2006. doi:10.1016/j.jcp.2005.04.027.
- [25] J. Perdew, K. Burke, and M. Ernzerhof. Generalized Gradient Approximation Made Simple. *Phys. Rev. Lett.*, 77:3865–3868, 1996. doi:10.1103/PhysRevLett.77.3865.
- [26] S. E. Pratsinis and P. T. Spicer. Competition between gas phase and surface oxidation of TiCl₄ during synthesis of TiO₂ particles. *Chem. Eng. Sci.*, 53:1861–1868, 1998. doi:10.1016/S0009-2509(98)00026-8.
- [27] S. E. Pratsinis, H. Bai, P. Biswas, M. Frenklach, and S. V. R. Mastrangelo. Kinetics of titanium(IV) chloride oxidation. *J. Am. Ceram. Soc.*, 73:2158–2162, 1990. doi:10.1111/j.1151-2916.1990.tb05295.x.
- [28] R. Raghavan. *Measurement of the High-Temperature Kinetics of Titanium Tetrachloride (TiCl₄) Reactions in a Rapid Compression Machine*. PhD thesis, Case Western Reserve University, <http://www.case.edu/cse/eche/people/students/theses/RaghavanRam-PhD.pdf>, August 2001.
- [29] M. Ramamoorthy, D. Vanderbilt, and R. D. King-Smith. First-principles calculations of the energetics of stoichiometric TiO₂ surfaces. *Phys. Rev. B*, 49(23):16721–16727, Jun 1994. doi:10.1103/PhysRevB.49.16721.
- [30] M. Rasmussen, L. Molina, and B. Hammer. Adsorption, diffusion, and dissociation of molecular oxygen at defected TiO₂ (110): A density functional theory study. *J. Chem. Phys.*, 120(2):988–997, 2004. doi:10.1063/1.1631922.
- [31] R. Schaub, P. Thostrup, N. Lopez, E. Lægsgaard, I. Stensgaard, J. K. Nørskov, and F. Besenbacher. Oxygen vacancies as active sites for water dissociation on rutile TiO₂ (110). *Phys. Rev. Lett.*, 87(26):266104, Dec 2001. doi:10.1103/PhysRevLett.87.266104.
- [32] R. Shirley, Y. Liu, T. S. Totton, R. H. West, and M. Kraft. First-principles thermochemistry for the combustion of a TiCl₄ and AlCl₃ mixture. *J. Phys. Chem. A*, 113(49):13790–13796, 2009. doi:10.1021/jp905244w.

- [33] R. Shirley, M. Kraft, and O. R. Inderwildi. Electronic and optical properties of aluminium-doped anatase and rutile TiO₂ from ab initio calculations. *Phys. Rev. B*, 81(7):075111, Feb 2010. doi:10.1103/PhysRevB.81.075111.
- [34] R. Shirley, W. Phadungsukanan, M. Kraft, J. Downing, N. E. Day, and P. Murray-Rust. First-principles thermochemistry for gas phase species in an industrial rutile chlorinator. *The Journal of Physical Chemistry A*, 114(43):11825–11832, 2010. doi:10.1021/jp106795p. URL <http://pubs.acs.org/doi/abs/10.1021/jp106795p>.
- [35] R. D. Smith, R. A. Bennett, and M. Bowker. Measurement of the surface-growth kinetics of reduced TiO₂(110) during reoxidation using time-resolved scanning tunneling microscopy. *Phys. Rev. B: Condens. Matter Mater. Phys.*, 66(3):035409, Jul 2002. doi:10.1103/PhysRevB.66.035409.
- [36] D. C. Sorescu and J. T. Yates. Adsorption of CO on the TiO₂ (110) surface: A theoretical study. *The Journal of Physical Chemistry B*, 102(23):4556–4565, 1998. doi:10.1021/jp9801626. URL <http://pubs.acs.org/doi/abs/10.1021/jp9801626>.
- [37] P. T. Spicer, O. Chaoul, S. Tsantilis, and S. E. Pratsinis. Titania formation by TiCl₄ gas phase oxidation, surface growth and coagulation. *J. Aerosol Sci.*, 33:17–34, 2002. doi:10.1016/S0021-8502(01)00069-6.
- [38] T. S. Totton, R. Shirley, and M. Kraft. First-principles thermochemistry for the combustion of TiCl₄ in a methane flame. *Proceedings of the Combustion Institute*, 33(1):493–500, 2011. ISSN 1540-7489. doi:10.1016/j.proci.2010.05.011. URL <http://www.sciencedirect.com/science/article/B7GWS-50RFN1X-9/2/d10e70fc1826457defc0707c90c13b17>.
- [39] S. Tsantilis and S. E. Pratsinis. Narrowing the size distribution of aerosol-made titania by surface growth and coagulation. *J. Aerosol. Sci.*, 35:405–420, 2004. doi:10.1016/j.jaerosci.2003.09.006.
- [40] R. A. van Santen and J. W. Niemantsverdriet. *Chemical kinetics and catalysis*. Plenum Press, 1995.
- [41] D. Vanderbilt. Soft self-consistent pseudopotentials in a generalized eigenvalue formalism. *Phys. Rev. B*, 41(11):7892–7895, Apr 1990. doi:10.1103/PhysRevB.41.7892.
- [42] C. G. Wells, N. M. Morgan, M. Kraft, and W. Wagner. A new method for calculating the diameters of partially-sintered nanoparticles and its effect on simulated particle properties. *Chem. Eng. Sci.*, 61(1):158–166, 2006. doi:10.1016/j.ces.2005.01.048.
- [43] S. Wendt, R. Schaub, J. Matthiesen, E. Vestergaard, E. Wahlström, M. Rasmussen, P. Thostrup, L. Molina, E. Lgsgaard, I. Stensgaard, B. Hammer, and F. Besenbacher. Oxygen vacancies on TiO₂(110) and their interaction with H₂O and O₂: A combined high-resolution stm and dft study. *Surface Science*, 598(1-3):226–245, 2005. ISSN 0039-6028. doi:10.1016/j.susc.2005.08.041.

URL <http://www.sciencedirect.com/science/article/B6TVX-4HDP8PP-2/2/d0b999c4eb2725760671e663af8b9a74>.

- [44] R. H. West, G. J. O. Beran, W. H. Green, and M. Kraft. First-principles thermochemistry for the production of TiO_2 from TiCl_4 . *J. Phys. Chem. A*, 111(18):3560–3565, 2007. doi:10.1021/jp0661950.
- [45] R. H. West, M. S. Celnik, O. R. Inderwildi, M. Kraft, G. J. O. Beran, and W. H. Green. Toward a comprehensive model of the synthesis of TiO_2 particles from TiCl_4 . *Ind. Eng. Chem. Res.*, 46(19):6147–6156, 2007. ISSN 0888-5885. doi:10.1021/ie0706414.
- [46] R. H. West, R. Shirley, M. Kraft, C. F. Goldsmith, and W. H. Green. A detailed kinetic model for combustion synthesis of titania from TiCl_4 . *Combust. Flame*, 156: 1764–1770, 2009. doi:10.1016/j.combustflame.2009.04.011.